THE JOURNAL OF BIOLOGICAL CHEMISTRY VOL. 283, NO. 45, pp. 30522–30530, November 7, 2008

OSTM1 Bone Defect Reveals an Intercellular Hematopoietic Crosstalk*[S]

Received for publication, July 10, 2008, and in revised form, September 8, 2008 Published, JBC Papers in Press, September 11, 2008, DOI 10.1074/jbc.M805242200

Monica Pata, Céline Héraud, and Jean Vacher[1]

From the Department of Cellular Interactions and Development, Institut de Recherches Cliniques de Montréal, Faculté de Médecine de l'Université de Montréal, Québec H2W 1R7, Canada

The most severe form of bone autosomal recessive osteopetrosis both in humans and in the gray-lethal (*gl/gl*) mouse is caused by mutations in the *Ostm1* gene. Although osteopetrosis is usually associated with a defect in the hematopoietic-derived osteoclast cells, this study determined that *Ostm1* is expressed in many hematopoietic cells of the myeloid and lymphoid B- and T-lineages. Hematopoiesis in *gl/gl* mice is characterized by a marked expansion of the osteoclast lineage but also by deregulation of the lymphoid lineages with a decrease in B-lymphoid cell populations and altered distribution in T-lymphoid double and single CD4 CD8-positive cells. In committed *gl/gl* osteoclasts, specific *Ostm1* transgene targeting showed a requirement of additional factors and/or cells for normal osteoclast function, and importantly, defined the *gl* osteopetrotic defect as non-cell autonomous. By contrast, *gl/gl* osteoclast, B- and T-lymphoid lineage phenotypes were rescued when *Ostm1* is expressed under PU.1 regulation from a bacterial artificial chromosome transgene, which established an essential role for *Ostm1* in hematopoietic cells in addition to osteoclasts. Together these experiments are the first to demonstrate the existence of hematopoietic crosstalk for the production of functional and active osteoclasts.

A strict balance between bone formation and resorption in vertebrates is required throughout adult life to maintain a constant bone mass (1–3). The cells responsible for bone resorption are the osteoclasts that are formed through the fusion of hematopoietic myeloid cells. Failure of appropriate hematopoietic progenitors to differentiate or to mature into functional osteoclasts results in abnormal accumulation of mineralized osteoid and leads to osteopetrosis (4).

Severe human osteopetrosis is characterized by dense sclerotic bone, accumulation of mineralized osteoid and cartilage (5–8), and causes drastic reduction of bone marrow (1, 9). Associated with the limited bone marrow compartment, patients display defective hematopoiesis with anemia, thrombocytopenia, high susceptibility to infections, and die at a young age. The only therapy for severe cases of osteopetrosis is bone marrow transplantation (10, 11). Allogeneic bone marrow transplantation is possible for these patients, but this approach has major limitations. Alternatively, autologous hematopoietic stem cell transplantation upon gene therapy correction could circumvent these drawbacks. However, development of gene therapy protocols requires proper knowledge of hematopoiesis in osteopetrotic disorders.

At present only mutation in *OSTM1* and in three other genes, *TCIRG1*, *ClCN7*, and *RANKL* have been directly associated with severe autosomal recessive osteopetrosis in human (12–16). The human *OSTM1* gene has been characterized, and *OSTM1* patients display the most severe recessive osteopetrotic phenotype and die at early ages (17–19).

Osteopetrotic mouse mutations have been characterized and associated with osteoclast differentiation or activation defects, including numerous transcription factors, such as PU.1, that play a crucial role in osteoclast lineage differentiation (20), as well as proteins important in osteoclast activation, the murine *Ostm1* (21). This murine *Ostm1* gene was first identified in the gray-lethal (*gl*)[2] mouse mutant (17) and encodes a unique transcript. Based on protein structural analysis, the Ostm1 protein likely corresponds to a type I transmembrane protein (17). The *gl* mutation consists of a deletion that results in a null phenotype with absence of transcript and protein expression. *gl* mice produce osteoclasts, defined by multinucleated cells positive for the classic TRAP marker, but which are functionally inactive (21). Interestingly, *gl* mice demonstrated a significant increase in the mature bone-resident osteoclast population (21). Although the osteoclast defects in *gl* mice have been well analyzed histologically and *ex vivo*, it is important for the design of appropriate therapeutic approaches, for example autologous gene therapy, to understand the fundamental hematopoietic cellular defects and the role of *Ostm1* in hematopoietic lineage differentiation and maturation.

This study first characterized, in *gl/gl* hematopoietic phenotypes, an expansion of the osteoclast lineage as a compensatory mechanism and major lymphopoiesis anomalies with reduced B-lymphoid cell population and altered T-lymphoid cell differentiation pattern. Second, our results on Ostm1 hematopoietic-targeted transgenic mice support that Ostm1 is required not

* This work was supported by Canadian Institutes of Health Research and National Sciences and Engineering Council of Canada grants (to J. V.). The costs of publication of this article were defrayed in part by the payment of page charges. This article must therefore be hereby marked "*advertisement*" in accordance with 18 U.S.C. Section 1734 solely to indicate this fact.

[S] The on-line version of this article (available at http://www.jbc.org) contains supplemental Table S1 and Fig. S1.

[1] To whom correspondence should be addressed: Institut de Recherches Cliniques de Montréal, 110, Avenue des Pins West, Montréal, Québec H2W 1R7, Canada. Tel.: 514-987-5734; Fax: 514-987-5585; E-mail: vacherj@ircm.qc.ca.

[2] The abbreviations used are: *gl*, gray-lethal mouse; BAC, bacterial artificial chromosome; TRAP, tartrate-resistant acid phosphatase; OCLs, osteoclast-like cells; FACS, fluorescence-activated cell sorting; hGH, human growth hormone; CFU-E, erythroid colony-forming units; CFU-GM, granulocyte-macrophage CFUs; CFU-M, macrophage CFUs; CFU-GEMM, granulocyte, erythroid, macrophage, and megakaryocyte CFUs.

only in osteoclast lineage but also in other lineages to fully rescue *gl/gl* osteopetrosis and defective hematopoiesis.

MATERIALS AND METHODS

Mice

The mouse strain GL/Le *dl*^{J} +/+*gl* was obtained from The Jackson Laboratory (Bar Harbor, ME) and maintained by heterozygous brother × sister mating for ~150 generations. Homozygous *gl/gl* mice used for analysis had a healthy appearance. Experiments with animals complied and were approved by the institutional animal care committee and Canadian Committee for Animal Protection.

Production and Analysis of Transgenic Mice

TRAP-Ostm1—The TRAP-*Ostm1* construction was produced with the *Ostm1* cDNA (1.055 kb) linked to the TRAP promoter (1.8 kb, XhoI/XbaI) upstream (22), and to the human hGH poly(A) signal (2.1 kb) downstream. Linearized transgene (XhoI/NotI) was injected into fertilized oocytes from F2 (C3H × C57BL/6) (23). Transgenic mice were identified by PCR with TRAP forward (5′-GTCCTCACCAGAGACTCTGAAC-3′) and Ostm1 reverse (5′-CAAGTCCTGCACCTCCAACAG-3′) primers. PCR amplification conditions were 94 °C, 5 min, followed by 30 cycles of 94 °C for 0.5 min, 65 °C for 0.5 min, and 72 °C for 0.5 min. Transgene integrity and copy number were determined by Southern analysis. Each transgenic line was successively crossed with heterozygous *gl*/+ mice to generate *gl/gl* TRAP-*Ostm1* transgenic progenies.

PU.1-Ostm1—Three PU.1 BAC clones were first isolated from a 129Sv mouse pBelo11 BAC genomic library (Research Genetics). These BAC clones contained, based on two PCR assays, >19 kb of upstream regulatory sequences of PU.1 with primers at ~−19 kb (forward, 5′-TCTTGAATGCCTGCTTGTG-3′; reverse, 5′-TTGGAGCTGGAGAGATGGTTC-3′) and the PU.1 second exon with another primer set (forward, 5′-CGGATGACTTGGTTACTTACG-3′; reverse, 5′-GGGCTGACATTGTGTGGATAC-3′). From pulse field gel electrophoresis, Southern blot, and end-junction sequencing analysis, one of these BAC clones (~100 kb) was selected for further experiments and contained >30 kb of PU.1 regulatory sequence, the full-length *PU.1* gene as well as the *Tbp1* gene.

Two targeting constructs for homologous recombination were produced in pLD53.SC1 BAC recombination vector to modify the original PU.1 BAC clone. The first construct was designed to delete the *Tbp1* gene from the original BAC. Two homologous regions on each side of the *Tbp1* gene, 31 kb apart, were PCR-amplified from PU.1 BAC DNA and cloned in pLD53.SC1 vector (24). The second construct was designed to replace the PU.1 genomic sequence by the *Ostm1* open reading frame and an in-frame iEGFP-PGK poly(A) sequences (1.7 kb). Homologous PU.1 5′ and 3′ regions were amplified from the original PU.1 BAC DNA and inserted upstream and downstream of the *Ostm1*-pA cloned in the pLD53.SC1 vector (supplemental Table S1).

Each of the two homologous constructs was used in a two-step RecA strategy for BAC modifications (24). The *Tbp1* gene was excised from the original PU.1 BAC creating the new BAC PU.1Δ*Tbp1*. The PU.1 genomic coding sequences were then replaced by those of *Ostm1* in the BAC PU.1Δ*Tbp1*, generating the PU.1-*Ostm1* BAC. At each step, the new BACs were fully characterized by pulse field gel electrophoresis and Southern blot. Modified *Tbp1* and *PU.1* regions were sequenced to verify proper gene deletion/substitution and exclude other alterations. The resulting PU.1-*Ostm1* BAC (~70 kb) was microinjected (17), and transgenic founders were identified by PCR using PU.1 forward (5′-GCCTTTCTCCCTCCCAGCC-3′) and Ostm1 reverse (5′-CAAGTCCTGCACCTCCAACAG-3′) primers. PCR amplification conditions were 94 °C, 5 min, followed by 30 cycles of 94 °C for 0.5 min, 65 °C for 0.5 min, and 72 °C for 0.5 min, and transgene integrity and copy number were determined by Southern blot. Each founder was successively crossed with heterozygous *gl*/+ mice to generate *gl/gl* PU.1-*Ostm1* transgenic progenies.

Cellular Analysis

Hematologic Parameters—Blood from *gl/gl* and control mice was obtained by cardiac puncture and collected into EDTA-coated tubes (BD Microtainer). Hematological analysis was performed using a Bayer Advia 120 automated cell analyzer with the mouse archetype of multispecies software version 2.206 (CBTR, Montreal, Canada). The spleen and thymus were monitored as percentage of organ to total body weight.

FACS Analysis—Flow cytometric analyses were carried out on spleen, thymus, and bone marrow single cell suspension in phosphate-buffered saline with 1% heat-inactivated fetal bovine serum. Nucleated cells (1.5×10^6) were stained with phycoerythrin-conjugated CD11b, B220, IgD, or CD4 (Pharmingen) and with fluorescein isothiocyanate-conjugated IgM, CD5, Ly6-G, CD8, and CD11c (Cedarlane). Samples were analyzed on a BD FACSCalibur four-color flow cytometer with System II software.

Hematopoietic Progenitor Clonogenic Assays—The number of splenic nucleated cells was quantified from single cell suspension in Iscove's modified Dulbecco's medium containing 1% methylcellulose, 10% fetal calf serum, erythropoietin (1.0 unit/ml), murine IL-3 (0.8% v/v of WEHI-3 supernatant), 1% bovine serum albumin, transferrin (190 mg/ml), and α-monothioglycerol (5×10^{-2} M) (25). Each assay was set up in triplicates, and colony-forming units were defined by morphology, size (cell number), and hemoglobinization. Erythroid colony-forming units (CFU-E) were counted at day 2, whereas burst-forming units (BFU-E), granulocyte-macrophage colony-forming units (CFU-GM), and macrophage colony-forming units (CFU-M) were counted at day 7 and granulocyte, erythroid, macrophage, and megakaryocyte colony-forming units (CFU-GEMM) at day 11.

Ex Vivo Osteoclast Differentiation—Bone marrow-derived macrophage cells were generated *ex vivo* from bone marrow cells cultured for 5 days in α-minimal essential medium supplemented with 10% fetal bovine serum and macrophage-colony-stimulating factor. Osteoclast-like cells (OCLs) were generated from bone marrow-derived macrophage cell differentiation *in vitro* for 6 days in α-minimal essential medium supplemented with 10% fetal bovine serum, 10 ng/ml macrophage-colony-stimulating factor, and 50 ng/ml receptor activator of NF-κB ligand. Alternatively, OCLs were generated *ex vivo* by co-cul-

ture of primary calvaria osteoblasts with bone marrow/spleen cells as previously described (21).

Expression Analysis

Total RNA from OCLs, enriched hematopoietic cells, and tissues, including bone marrow, brain, kidney, thymus, liver, and spleen, were isolated with TRIzol (Invitrogen). TRAP-*Osmt1* transgene expression was determined by semi-quantitative PCR on 0.5 μg of total RNA. The primers used were: *Ostm1* endogenous forward 5′-CCTGCTTTGAGCATAACCTGA-3′ (*Ostm1* exon 3) and reverse 5′-CTGCAGTCCCAACATTTCGTGAG-3′ (*Ostm1* 3′-untranslated region); TRAP-*Ostm1* transgene, forward 5′-GTGGTTGCTGTGTCTGTGTTCA-3′ (*Ostm1* exon 5), reverse 5′-TTGGGATATAGGCTTCTTCAAACTC-3′ (hGH); *Trap* gene forward 5′-TGTTCTCTGACCGTGCCCTTC-3′ (*Trap* exon 3) and reverse 5′-CCCACTCAGCACATAGCCCCA-3′ (*Trap* exon 5). PCR conditions were 94 °C for 5 min, followed by 30 cycles of 94 °C for 0.5 min, 65 °C for 0.5 min, and 72 °C for 0.5 min.

PU.1-*Ostm1* transgene expression was determined by real-time quantitative PCR on 0.1 μg of DNase (Invitrogen)-treated total RNA. The primers used were for *Ostm1* endogenous forward 5′-GCTTCCTTCACTCAGAGCAA-3′ (*Ostm1* exon 5) and reverse 5′-GTGAGAATGCAACTTGTCCGA-3′ (*Ostm1* exon 6); PU.1-*Ostm1* transgene, forward 5′-GCTTCCTTCACTCAGAGCAA-3′ (*Ostm1* exon 5), reverse 5′-AGTGAATAGGAACTTCGGAA-3′(EGFP); *Trap* forward 5′-GGTATGTGCTGGCTGGA-3′ (*Trap* exon 3) and reverse 5′-GACTGGCAAAGTCATCTGA-3′ (*Trap* exon 5); *PU.1* endogenous forward 5′-ATGGAGCTGGAACAGATGCA-3′ (*PU.1* exon 3) and reverse 5′-CCAAGCCATCAGCTTCTCCA-3′ (*PU.1* exon 4); *S16* forward 5′-GCTACCAGGGCCTTTGAGATG-3′ and reverse 5′-AGGACGGATTTGCTGGTGTGG-3′. All reactions were performed in triplicate in a Syber Green Master Mix (Qiagen). PCR conditions were 94 °C, 15 min, followed by 50 cycles of 94 °C for 0.5 min, 55 °C for 0.5 min, and 72 °C for 0.5 min in an MX4000 Mutiplex quantitative PCR analyzer.

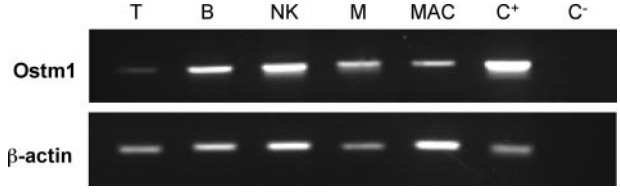

FIGURE 1. **Ostm1 expression in hematopoietic cells.** Semi-quantitative Ostm1 expression from enriched hematopoietic cells detected high levels in B-lymphocyte (*B*), natural killer (*NK*), mast (*M*) cells and lower expression in T-lymphocyte (*T*) and activated macrophage (*MAC*) in comparison to positive brain tissue control (C^+), negative control (C^-), and normalized to β-actin.

Histological and X-ray Analysis

Bone samples from 3-week-old mice were fixed in 10% phosphate-buffered formalin, decalcified in 0.5 M EDTA, and embedded in paraffin. Sections were stained with hematoxylin and eosin (H&E), mounted, and analyzed. X-ray scan was carried out using Faxitron MX20 (18 Kv, 10 s).

Statistical Analysis

Values are expressed as mean ± S.D. Unpaired two-sample Student's *t* test was used for statistical analysis with $p < 0.05$ considered significant.

RESULTS

Ostm1 Expression in Several Mature Hematopoietic Cell Populations

Ostm1 expression profile was determined in wild-type mature hematopoietic cells derived from myeloid and lymphoid populations. Enriched *ex vivo* hematopoietic cell populations were obtained from cultured C57BL/6J spleen, bone marrow, and peritoneal cavity cells (26, 27). Semi-quantitative expression analysis of endogenous Ostm1 showed high levels in B, NK, and mast cells and lower levels in T cells and activated macrophages relative to actin control (Fig. 1), suggesting that Ostm1 could play a role in several hematopoietic cell types.

Altered Hematology and Hematopoiesis in gl/gl Mice

Anemia and Leukopenia in gl/gl Mice—To determine the impact of the *gl* mutation on hematopoietic cell populations, we evaluated hematological parameters of *gl/gl* and wild-type control littermates. The *gl/gl* mice showed a significant reduction in the number of red blood cells compared with wild-type mice, as well as a significant reduction in hematocrit and hemoglobin indicating a mild anemia (Table 1). In parallel, the number of white blood cells and lymphocytes was significantly decreased, indicating leukopenia and lymphopenia in *gl/gl* mice (Table 1). Homozygous *gl/gl* mice displayed a spleen to body weight ratio comparable to wild-type mice despite anemia (Table 2). Consistently, histological examination of the spleen did not show any profound architectural alteration of the white or red pulps where B cell maturation and myelopoiesis occur respectively (data not shown).

Analysis of Myeloid Lineages: Stimulation of gl Osteoclast Progenitors—Since *gl/gl* mice exhibit altered hematological parameters, spleen hematopoietic progenitor populations of homozygous *gl/gl* mice were evaluated using clonogenic assays, because there is a massive depletion of bone marrow cells in this severe osteopetrotic phenotype. The level of multipotent CFU-GEMM cell population in *gl/gl* and age-matched control litter-

TABLE 1
Hematological parameters of grey-lethal (*gl/gl*) mice
Data are expressed as the means ± S.D.

Mice	*n*	RBC	Hematocrit	Hemoglobin	WBC	Lymphocytes	Monocytes	PLT
		10^9 cells/ml	%	g/dl	10^6 cells/ml	10^6 cells/ml	10^4 cells/ml	10^6 cells/ml
+/+	10	6.3 ± 1.7	34.1 ± 8.9	10.0 ± 2.7	4.1 ± 0.9	3.2 ± 0.6	11.1 ± 6.5	1000 ± 460
gl/gl	9	4.2 ± 2.1[a]	22.0 ± 10.7[b]	6.2 ± 2.8[b]	2.8 ± 1.7[a]	1.6 ± 1.3[c]	11.4 ± 6.5	707 ± 586

[a] $p < 0.05$.
[b] $p < 0.02$.
[c] $p < 0.001$.

TABLE 2

Altered hematopoietic progenitors in spleen of grey-lethal (*gl/gl*) mice

Data are expressed as the means ± S.D.

Mice	*n*	Body weight	Spleen weight	Spleen/body WT	Nucleated cell	*n*	CFU-E	BFU-E	CFU-GM	CFU-M	CFU-GEMM
		g	*g*	*%*	*(×10⁶/spleen)*		*×10²*	*×10²*	*×10²*	*×10²*	*×10²*
+/+	10	13.0 ± 2.4	0.096 ± 0.007	0.72	80.1 ± 3.6	3	298 ± 50	75 ± 10	61 ± 9	32 ± 7	3.9 ± 2
gl/gl	9	6.1 ± 1.3[a]	0.051 ± 0.017[a]	0.84	70.6 ± 9.4	3	287 ± 20	87 ± 11	147 ± 10[a]	33 ± 6	2.9 ± 1.3

[a] $p < 0.05$.

TABLE 3

Altered splenic myeloid and lymphoid cell populations of grey-lethal (*gl/gl*) mice

Data are expressed as the means % ± S.D.

Mice	*n*	Myeloid lineage		Lymphoid lineages				
		$CD11b^+$	$CD11b^+Ly6\text{-}G^+$	$B220^+ IgM^+$	$IgM^+ IgD^+$	$CD5^+$	$CD4^+$	$CD8^+$
+/+	6	3.7 ± 0.3	1.3 ± 0.2	23.1 ± 1.9	16.1 ± 2.5	9.2 ± 1.8	6.1 ± 1.4	3.1 ± 0.9
gl/gl	6	8.7 ± 2.2[a]	5.9 ± 2.5[a]	13.4 ± 1.6[a]	12.4 ± 1.6[a]	7.5 ± 1.2	9.4 ± 3.0	6.5 ± 2.6

[a] $p < 0.001$.

TABLE 4

Thymus analysis and altered distribution in cell populations of grey-lethal (*gl/gl*) mice

Data are expressed as the means % ± S.D.

Mice	*n*	Body weight	Thymus weight	Thymus/body WT	Nucleated cells	$CD4^+CD8^+$	$CD4^+$	$CD8^+$
		g	*g*	*%*	*×10⁶/thymus*			
+/+	4	13.5 ± 2.1	0.058 ± 0.001	0.45	86.8 ± 13	80.5 ± 6.4	11.7 ± 5.1	5.1 ± 1.2
gl/gl	4	5.7 ± 1.0[a]	0.020 ± 0.003[a]	0.35[b]	10.5 ± 2.2[a]	9.5 ± 4.1[a]	63.7 ± 5.0[a]	21.7 ± 6.3[a]

[a] $p < 0.001$.
[b] $p < 0.05$.

mate mice was not significantly affected (Table 2). Similarly, erythroid differentiation potential quantified by early BFU-E and late CFU-E spleen progenitor cell populations in *gl/gl* mice showed, despite the anemia, no significant increase relative to age-matched controls (Table 2). In contrast, all *gl*/*gl* mice showed a marked 2.5-fold expansion of granulocyte-macrophage progenitors (CFU-GM), from which osteoclasts are derived, relative to wild-type control (Table 2). The size of CFU-GM colonies in *gl*/*gl* mice compared with control mice appeared larger, but maintained similar morphology. In addition, the levels of the CFU-M progenitor cells, from which macrophages are derived, were comparable in *gl*/*gl* and control mice, indicating that only the CFU-GM are affected.

To further characterize and quantify the osteoclast cell populations, we performed flow-cytometric analysis (FACS) on spleen cell populations using $CD11b^+$ and $Ly6\text{-}G^+$ antibodies. As shown in Table 3, the analysis revealed a significant increase of splenic $CD11b^+$ and $CD11b^+/Ly6\text{-}G^+$ cells that include osteoclast, macrophage, monocyte, and granulocyte populations in *gl/gl* mice relative to controls. In fact, the $CD11b^+/Ly6\text{-}G^+$ cell subpopulation was elevated ~4-fold in homozygous *gl*/*gl* mice, consistent with increased CFU-GM progenitors (Table 2). By contrast, analysis of the population of splenic dendritic $CD11b^+/CD11c^+$ cells was unchanged in *gl*/*gl* mice (data not shown).

Impaired gl Lymphopoiesis—Because homozygous *gl/gl* mice have reduced white blood cell count and human osteopetrotic patients have higher susceptibility to infections possibly due to altered immune response, the lymphoid lineages were investigated in *gl*/*gl* spleen and thymus. Quantification of the "late" B-lymphoid cell population by FACS revealed a significant decrease of ~40% of the $B220^+/IgM^+$ cell population in the *gl*/*gl* mice compared with control. Similarly, the more mature IgM^+/IgD^+ cell population was also significantly reduced in *gl/gl* mice (Table 3). Because the B-lymphoid compartment is constituted of two distinct B1 and B2 cell populations (28), we have quantified the B1 cell population separately using the specific CD5 (Ly-1) marker to monitor B-cell differentiation potential. In *gl*/*gl* mice, the B1 self-renewing cells ($CD5^+$) that differentiate independently from bone marrow stroma were slightly reduced (~18%) relative to control mice (Table 3).

The *gl/gl* thymus was consistently smaller in comparison to age-matched littermates and the ratio of thymus to body weight was significantly reduced (Table 4). Quantification of the major thymic T-cell populations in *gl/gl* and wild-type littermate animals showed altered thymic cellular subpopulations. Although the *gl/gl* double negative $CD4^-CD8^-$ cell subpopulation was unchanged, an important depletion in the double positive $CD4^+CD8^+$ subpopulation was determined relative to wild type (Table 4). Concurrently, the *gl/gl* mice displayed a major 4- to 5-fold increase in single CD4- and CD8-positive cells (Table 4), suggesting enhanced thymic cell maturation.

Non-cell Autonomous Ostm1 Role in Committed Osteoclast

In *gl/gl* mice, the increased progenitor and mature osteoclast population, concomitant with inactive osteoclasts (21), indicated that *Ostm1* expression was required in late committed precursors of the osteoclast lineage. To investigate this hypothesis, transgenic mice expressing *Ostm1* under the control of the committed osteoclasts TRAP gene promoter were generated (Fig. 2*A*). Three TRAP-*Ostm1* transgenic lines (2–10 transgene copies) were assessed for osteoclast-specific expression, precursor frequency, and differentiation potential. Expression of the transgene was slightly below endogenous expression in two lines (630 and 692), and above in one line (670) (Fig. 2*B*). Transgenic OCLs from all lines showed similar frequency

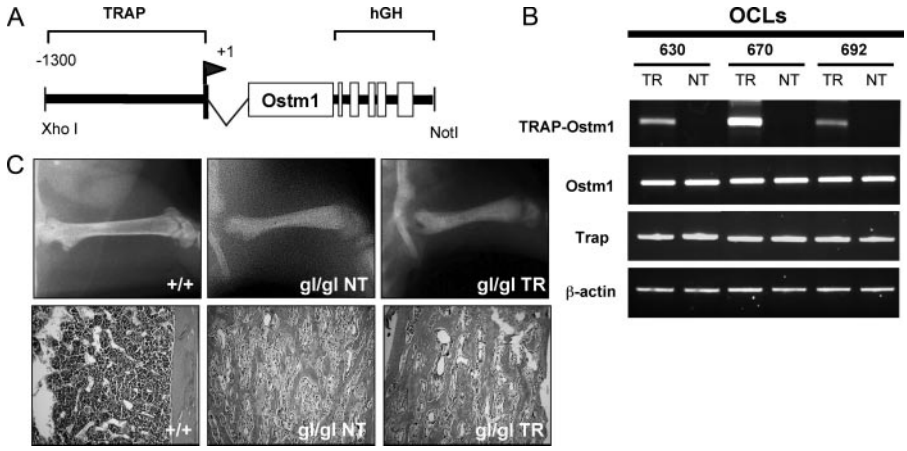

FIGURE 2. **Production, expression, and analysis of TRAP-Ostm1 transgenic mice.** *A*, schematic representation of the transgene used to generate TRAP-Ostm1 mice. The TRAP regulatory sequences (1.3 kb), transcription initiation site (+1), first exon (500 bp), and intron 1 were cloned upstream of Ostm1 (1.055 kb) open reading frame followed by the 3′ and poly(A) of human growth hormone gene (*hGH*; 2.1kb). *B*, transgene expression in OCLs (*TR*) from each TRAP-Ostm1 transgenic lines was compared with non-transgenic OCL controls (*NT*). Endogenous Trap, Ostm1, and β-actin expression were used as controls. *C*, persistence of osteopetrosis was observed in homozygous gl/gl TRAP-Ostm1 transgenic mice (*gl/gl TR*) similar to gl/gl non-transgenic littermate (*gl/gl NT*) in contrast to wild-type control (+/+) as detected by x-ray analysis (*top panels*) and on histological bone sections (*bottom panels*, magnification, ×50).

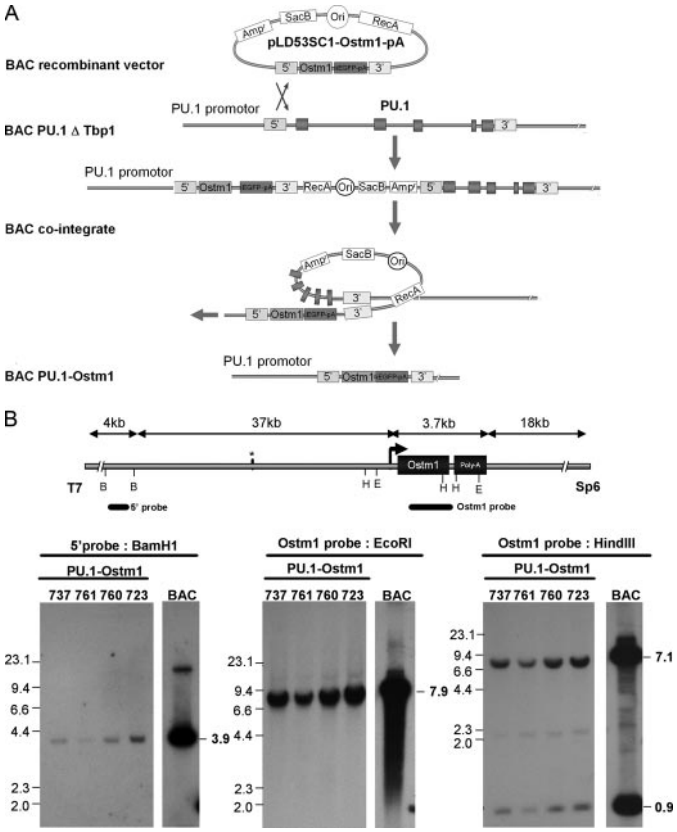

FIGURE 3. **Production and analysis of BAC PU.1-Ostm1 transgene.** *A*, schematic representation illustrates the BAC PU.1 ΔTbp1 to the BAC PU.1-Ostm1 recombination step. The PU.1 genomic sequences in BAC PU.1 ΔTbp1 were replaced by Ostm1-EGFP-poly(A) with pLD53-Ostm1-PA vector containing 5′ and 3′ PU.1 homology cassettes on each side of Ostm1-EGFP-pA. The BAC co-integrant recombination removed the pLD53.SC1 vector and produced the new BAC PU.1-Ostm1. *B*, the BAC PU.1-Ostm1 was used to generate transgenic lines. Southern blot of genomic DNA analysis with the following restriction digests are shown: *left panel*, BamHI (*B*) digest hybridized with a 5′ probe that detect a 3.9-kb band for the transgene; *middle* and *right panels*, EcoRI (*E*) or HindIII (*H*) hybridized with an Ostm1 probe (*exon1–exon6*) with one band at 7.9 kb for EcoRI digestion and two bands at 7.1 kb and 0.9 kb for HindIII digests for the transgene. Genomic DNA from the original BAC PU.1-Ostm1 was used as control.

and differentiation potential as non-transgenic OCLs (data not shown). Importantly, the TRAP-*Ostm1* transgenic mice did not exhibit any bone defects.

The TRAP-*Ostm1* transgenic mice from the three lines then served to test for osteopetrosis complementation by successive mating to heterozygous *gl*/+ mice. Transgenic *gl*/*gl* TRAP-*Ostm1* mice generated from these matings were genotyped for the *Ostm1* mutation (17) and the transgene. All *gl*/*gl* TRAP-*Ostm1* transgenic progenies displayed an osteopetrotic phenotype similar to *gl*/*gl* non-transgenic mice with reduced bone marrow space and lack of tooth eruption (Fig. 2*C*). This indicated that Ostm1 expression in committed osteoclast precursors to mature cells is not sufficient to rescue the *gl/gl* osteoclast defect.

gl Hematopoiesis/Osteopetrosis Correction by Ostm1 Expression in Multihematopoietic Cells

Lack of complementation in *gl/gl* TRAP-*Ostm1* transgenic mice and the multihematopoietic lineage defects in *gl/gl* mice suggested that Ostm1 expression is required in other hematopoietic cell or lineage at earlier stage. Because the PU.1 transcriptional factor is essential in the early osteoclast lineage as well as in several early hematopoietic progenitors, including erythropoietic and lymphoid lineages (20, 29), regulatory elements of the PU.1 (*Sfpi1*) gene were selected to target *Ostm1* expression in transgenic mice. A 100-kb PU.1 BAC clone was isolated that contains regulatory sequences with the CAAT/enhancer-binding protein-α enhancer binding site (30), localized 14 kb upstream of PU.1 essential for expression in transgenic mice (31–33). This PU.1 BAC was modified by homologous recombination. The first modification specifically deleted the adjacent *Tbp1* (*Pmsc3*) gene (~30 kb) to have exclusively PU.1 gene in the BAC. This PU.1-Δ*Tbp1* BAC was then subjected to a second round of recombination, to replace the PU.1 coding sequence by that of *Ostm1* (Fig. 3*A*). The resulting ~70 kb PU.1-*Ostm1* BAC clone contained ~37 kb of 5′ PU.1 regulatory sequence and 18 kb of 3′ sequence as determined by restriction pattern analysis and sequencing.

Four transgenic PU.1-*Ostm1* founders were generated carrying between 2 and 10 copies of the transgene. Transgene integrity in these lines (723, 737, 761, and 760) was monitored by analysis of vector/insert junctions and hybridization pattern with four specific probes (Fig. 3*B* and data not shown). Transgene quantitative expression was detected in spleen of all transgenic lines but at a much lower level compared with endogenous *Ostm1* in transgenic and in non-transgenic controls (Fig. 4*A*). In two representative lines, the spleen, bone marrow, and thymus displayed highest expression, whereas liver, kidney, and brain had lower levels (Fig. 4, *A* and *B*). In comparison to endog-

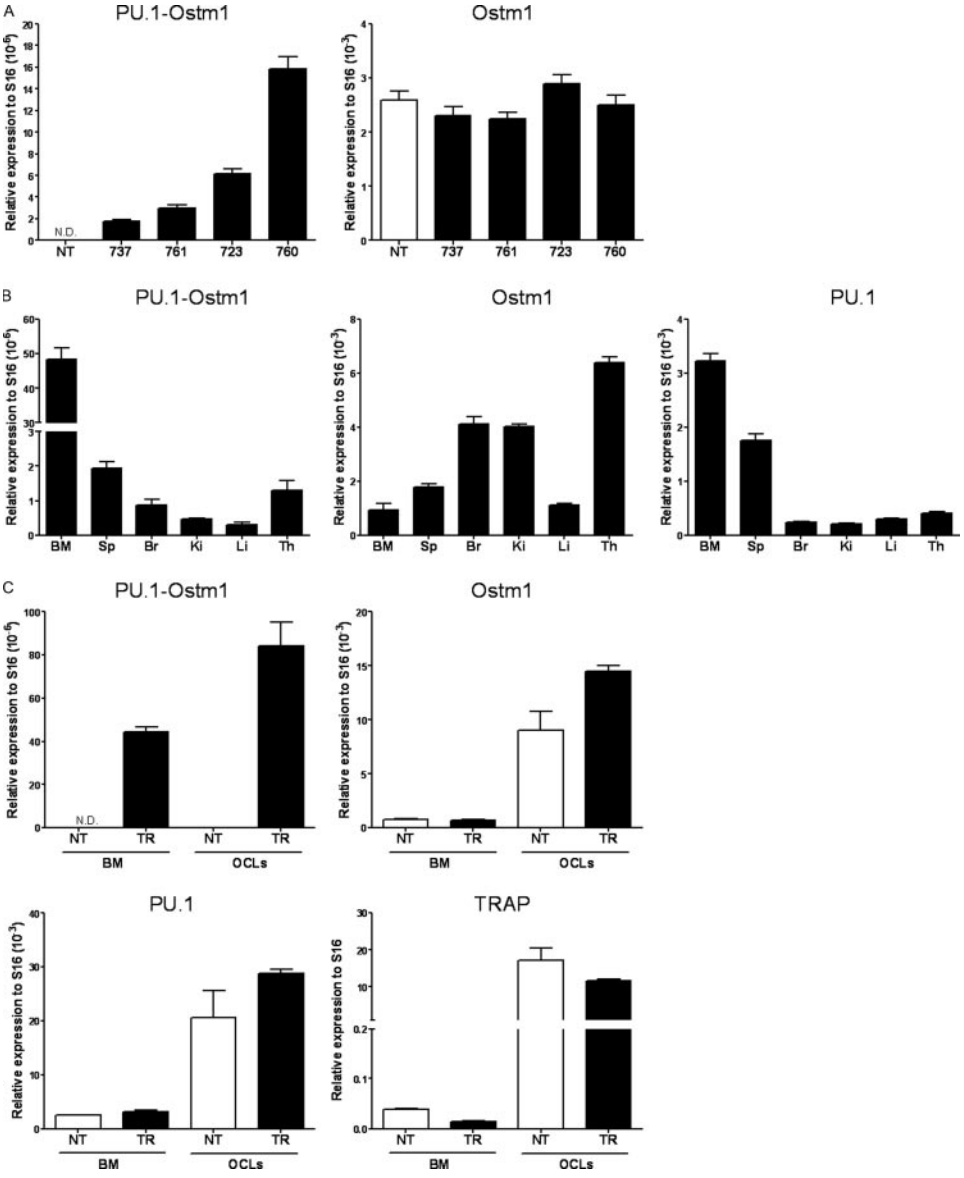

FIGURE 4. **Expression analysis of the PU. 1-Ostm1 transgene.** *A*, real-time quantitative spleen PU.1-Ostm1 transgene and endogenous *Ostm1* expression from the four PU.1-Ostm1 transgenic lines (*TR*) and non-transgenic (*NT*) was established relative to S16 as internal control. *B*, real-time quantitative PU.1-Ostm1 transgene and Ostm1, PU.1 endogenous genes expression was carried out on different tissues of PU.1-*Ostm*1 transgenic (*TR*) mice line #761 ($n = 3$) relative to S16 as internal control. High expression was detected in bone marrow (*BM*), spleen (*Sp*), and thymus (*Th*) and lower levels in brain (*Br*), liver (*Li*), and kidney (*Ki*). *C*, real-time quantitative transgene expression was performed on bone marrow (*BM*) and osteoclast like cells (*OCLs*) generated in culture from PU.1-*Ostm1* transgenic #737 (*TR*) and non-transgenic (*NT*) mice ($n = 3$) relative to S16 as internal control and compared with endogenous expression of Ostm1, PU.1, and TRAP.

enous *Ostm1* and *PU.1* expression, transgene expression levels were notably lower but displayed a similar expression pattern as PU.1 (Fig. 4, *A* and *B*). Transgene expression in bone marrow differentiated OCLs also showed *ex vivo* expression as observed for the endogenous Ostm1, PU.1, and TRAP controls (Fig. 4*C*). Notably, differentiated OCLs from transgenic PU.1-*Ostm1* bone marrow and spleen were produced at similar frequency as non-transgenic controls (data not shown). These transgenic mice did not develop any detectable phenotype.

To functionally monitor whether the PU.1-*Ostm1* transgene could rescue *gl/gl* osteopetrosis, three transgenic PU.1-*Ostm1* lines (737, 760, and 761) were successively mated to heterozygous *gl*/+ mice. Transgenic *gl/gl* PU.1-*Ostm1* mice from these matings were genotyped at the *Ostm1* locus and for the BAC transgene. Although non-transgenic homozygous *gl/gl* littermates exhibited the *gl* osteopetrotic phenotypes, all *gl/gl* transgenic progenies from the three lines tested displayed full tooth eruption and appropriate bone marrow development, providing evidence for functional rescue of osteoclastogenesis (Fig. 5).

To determine whether the entire spectrum of *gl/gl* hematopoiesis defects was corrected in *gl/gl* PU.1-*Ostm1* BAC transgenic mice, the myeloid and lymphoid cell populations of transgenic and age-matched non-transgenic *gl/gl* mice from two representative transgenic lines (737 and 761) were quantified by FACS analysis. In transgenic *gl/gl* PU.1-*Ostm1* mice, splenic $CD11b^+$ and $CD11b^+/Ly6\text{-}G^+$ cell populations showed levels similar to wild-type littermates, whereas these populations were significantly increased in homozygous *gl/gl* littermates (Table 5). Notably, correction of the myeloid population was obtained with both PU.1-*Ostm1* transgenic lines tested (Table 5). Analysis of transgenic bone marrow cell populations also showed control wild-type levels for the osteoclast lineage. In addition, the mature B cell populations in transgenic *gl/gl* PU.1-*Ostm1* evaluated in spleen and bone marrow returned to control levels in contrast to *gl/gl* mice. Interestingly, the thymic structure and the cellular distribution profile of single and double $CD4^+CD8^+$-positive T lymphoid cell populations in *gl/gl* PU.1-*Ostm1* transgenic were indistinguishable from controls (Table 5 and supplemental Fig. S1), indicating that the PU.1-*Ostm1* had fully rescued *gl/gl* thymic defect.

DISCUSSION

Ostm1 mutations lead to the most severe form of bone autosomal recessive osteopetrotic disorder in both humans and *gl/gl* mice and are associated with a defect in the hematopoietic osteoclast cell. Herein, Ostm1 analysis also uncovered expression in several myeloid and lymphoid lineages and when absent in *gl* mice resulted in altered hematopoietic differentiation and/or maturation with anemia, leukopenia, and lymphopenia. Char-

acterization of *Ostm1 in vivo* function by sole targeting to the *gl*/*gl* committed osteoclasts revealed the existence of additional factors or cells essential for osteoclast functional activation. Significantly, these findings established a non-cell autonomous mechanism for the *gl* defect. Moreover, complementation by early multilineage hematopoietic Ostm1 expression in *gl/gl* mice determined that Ostm1 is required in other hematopoietic cells, including osteoclast precursors, for full osteoclast function. Our studies demonstrated that Ostm1 plays a major role in myelopoiesis and lymphopoiesis and provided evidence of a crosstalk mechanism between hematopoietic cells for osteoclast activation.

Characterization of severe leukopenia and mild anemia in *gl/gl* mice pointed to defective hematopoietic differentiation. Such hematopoietic anomalies were likely downstream of the early hematopoietic multipotent CFU-GEMM progenitor stage, because this clonogenic population in *gl/gl* mice was unaffected. The unaltered erythroid lineage differentiation of the early BFU-E and late CFU-E progenitors argued that *gl* anemia results from hampered late erythropoiesis due to the severely reduced medullary space. By contrast, the *gl/gl* spleen CFU-GM, from which the osteoclasts are derived, were specifically increased while the more committed CFU-M progenitors, that give rise to macrophages but not to osteoclasts (34, 35), were unchanged. Further, a marked expansion of splenic early $CD11b^+/Ly6\text{-}G^+$ and late $CD11b^+$ osteoclast precursor stages in homozygous *gl*/*gl* indicated appropriate osteoclast lineage differentiation potential. This increase in osteoclast progenitors and precursors correlated with the presence of abundant mature *gl/gl* $TRAP^+$ osteoclasts (21). Such stimulation of cell populations throughout the *gl/gl* osteoclast lineage to the mature cells supports the existence of a compensatory mechanism in response to the inactive osteoclasts.

In addition to the osteoclast lineage expansion, the *gl/gl* lymphoid cell differentiation is altered. The reduced white blood cell counts in peripheral blood were consistent with decrease immature and mature B-lymphoid cell populations in *gl/gl* mice. Similar reduction in immature B-cells was observed previously in osteopetrosis, at least transiently at ~4 weeks of age, in the other osteopetrotic mice including *op*, c-*fos*, *oc*, and c-*src* mutants (36–38). Although these mutated genes have different functions and properties, it appears that reduced B-cell population is a hallmark of osteopetrosis and points to the absence of bone marrow microenvironment/compartment as a cause for this phenotype. However, the results of reduced B1 self-renewing cell population (CD5 marker) in *gl/gl* independently of the marrow and of the "conventional" splenic B cell population support the notion that the B-cell differentiation potential *per se* might be affected. Consequently, the B-cell phenotype in *gl/gl* mice may result from combined direct and indirect roles of Ostm1 in B-cell precursors and on bone microenvironment. Because B-cells normally produce osteoprotegerin, an inhibitor of osteoclastogenesis (39), such a decrease in B-cell population is likely to impinge on osteoprotegerin release and thereby be responsible for the increased osteoclast cell population of *gl/gl* mice. Similar to the B-cell population, the total *gl/gl* thymic T cell population was reduced and also displayed an altered distribution pattern. Indeed, the unchanged proportion of the immature *gl/gl* double negative $CD4^-CD8^-$ cell population compared with the depleted double positive $CD4^+CD8^+$ population implied that Ostm1 is very important during these differentiation stages. The subsequent significant increase in *gl/gl* mature CD4 and CD8 single positive cell populations con-

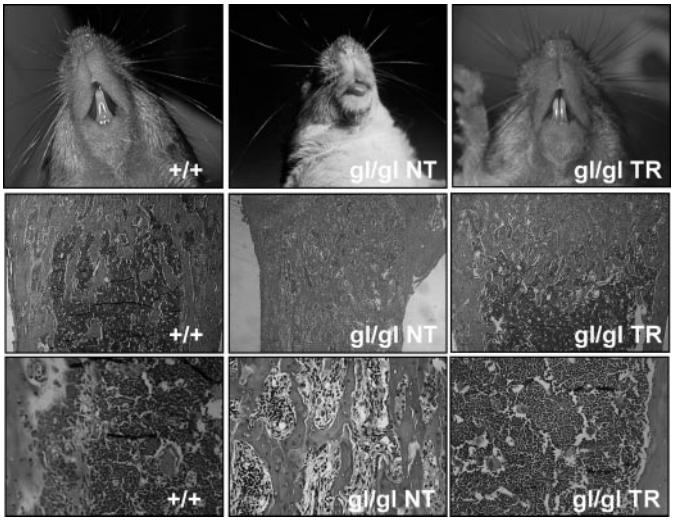

FIGURE 5. **Complementation of osteopetrosis in gl/gl PU. 1-Ostm1 transgenic mice.** Rescue of osteopetrosis in *gl/gl* PU.1-*Ostm1* transgenic (*gl/gl TR*) relative to non-transgenic (*gl/gl NT*) mice as shown by tooth eruption (*top panels*) and normal development of medullary space on bone sections stained with H&E (*middle* and *bottom panels*).

TABLE 5

Normalization of myeloid, B- and T-lymphoid cell populations in *gl/gl* PU.1-*Ostm1* transgenic mice

Data are expressed as the means % ± S.D. compared to wild type non-transgenic (+/+ NT).

Mice	*n*	Spleen			Bone marrow			*n*	Thymus			
		Myeloid lineage		B-lymphoid lineage	Myeloid lineage		B-lymphoid lineage					
		$CD11b^+$	$CD11b^+Ly6\text{-}G^+$	$B220^+$	$CD11b^+$	$CD11b^+Ly6\text{-}G^+$	$B220^+$		Nucleated cells × 10^6/thymus	$CD4^+CD8^+$	$CD4^+$	$CD8^+$
+/+ NT	6	11.5 ± 1.6	5.2 ± 2.0	61.9 ± 17.2	11.8 ± 3.1	21.1 ± 6.4	50.1 ± 9.3	6	70.6 ± 9.3	88.6 ± 3.8	7.0 ± 0.8	2.7 ± 1.4
+/+ TR	4	9.4 ± 4.9	4.3 ± 1.6	55.1 ± 14.2	9.7 ± 3.1	21.5 ± 7.3	51.4 ± 5.7	4	86.6 ± 17.4	89.0 ± 3.5	6.5 ± 1.6	2.8 ± 1.4
gl/gl NT	5	15.6 ± 2.0[a]	10.2 ± 4.7[a]	39.9 ± 8.9[b]	NA[c]	NA	NA	4	24.4 ± 7.0[d]	36.2 ± 13.1[a]	45.3 ± 20.4[b]	16.0 ± 7.2[b]
gl/gl TR 737	5	8.7 ± 1.2	4.0 ± 1.2	59.2 ± 6.3	10.0 ± 1.7	26.7 ± 4.5	47.2 ± 2.7	5	66.0 ± 9.3	87.6 ± 1.1	7.5 ± 1.3	3.4 ± 0.3
gl/gl TR 761	3	11.3 ± 1.5	4.2 ± 1.4	55.6 ± 7.8	14.9 ± 2.9	28.2 ± 1.8	41.0 ± 6.9	3	71.9 ± 8.7	89.4 ± 0.5	7.0 ± 0.2	2.3 ± 0.7

[a] $p < 0.005$.
[b] $p < 0.05$.
[c] NA, not applicable.
[d] $p < 0.001$.

trasted with the decrease in double positive cells, as detected in two osteopetrotic mice c-*fos* and *oc* (36, 37). This cellular differentiation pattern could be an indirect physiological response to maintain sufficient T-cell production. Alternatively, Ostm1 under normal conditions could slow down the positive selection mechanism of T-cell differentiation or, less likely, promote lymphocyte egression from the thymus (40). Together this hematopoietic characterization of *gl/gl* mice supports Ostm1 playing critical roles in multiple lineage differentiation at immature and/or mature cellular stages.

An important outcome from the study of transgenic Ostm1 expression in mice targeted to *gl/gl* committed and mature inactive osteoclasts was the absence of osteoclast correction. Despite substantial TRAP-*Ostm1* transgene expression in *gl/gl* mature osteoclasts, all *gl/gl* TRAP-*Ostm1* transgenic progenies displayed severe osteopetrosis similar to the *gl/gl* phenotype. This finding infers that the *gl* osteoclast defect is non-cell autonomous. Such data contrasts with another osteopetrotic phenotype caused by the ablation of the chloride channel ClC-7, a potential partner of Ostm1 in mature osteoclasts (41). In fact, re-expression of *Clcn7* with the same TRAP regulatory sequences in transgenic mice, as those used herein for Ostm1 on a $Clcn7^{-/-}$ background, was sufficient to produce active osteoclasts and rescue osteopetrosis (42). Our analysis indicates that the function of Ostm1 is not only in late osteoclastogenesis like CLC-7, but also in a wider hematopoietic cellular repertoire and implies a broader partner spectrum.

The complete hematopoietic rescue by the multilineage-targeted Ostm1 expression in PU.1 BAC transgenic of the *gl/gl* mice is compatible with a non-cell autonomous defect for the osteoclast and uncovered an essential role for Ostm1 in more than one hematopoietic cell type. Of significance, all *gl/gl* PU.1-*Ostm1* BAC transgenic mice demonstrated rescue of *gl/gl* osteopetrosis and hematopoietic defects even with a low level of transgene expression. This phenotypic correction provided additional and definitive evidence that *Ostm1* is the gene responsible for the *gl* defect. Most importantly, these results along with those of TRAP-*Ostm1* showed that Ostm1 expression in a cell(s) from the myeloid and/or lymphoid lineages contributes to correction of the osteoclast activation defect. In fact, involvement of more than one hematopoietic cell type in *gl* osteopetrosis is consistent with a previous rescue of *gl* phenotype by total bone marrow transplantation (43). To date no cell(s) other than osteoclasts, nor any underlying cellular process essential for osteoclast activation, have been described. Our experiments restricts the cell(s) essential for osteoclast resorptive function to those concomitantly expressing Ostm1- and PU.1-targeted cells that are early precursors, multipotent granulocyte-macrophage, pro-T, and/or pro B-cells (29, 44). Based on Ostm1 type I transmembrane structure, the cellular process likely implicates cell-cell interactions or secreted factors for osteoclast activation. Although several cytokines and chemokines secreted from hematopoietic cells (45, 46) and osteoblasts are critical for osteoclastogenesis, none have been shown physiologically or in cell culture to be necessary for osteoclast activation. Nevertheless, we propose that Ostm1 participates in a cell trafficking pathway with a partner repertoire of hematopoietic receptors and factors that will subsequently trigger a crosstalk mechanism for osteoclast activation. Based on this finding, autologous gene therapy for osteopetrosis will require adapted strategy design targeted to several hematopoietic lineages for correction of the disease.

In summary, loss-of-function of Ostm1 resulted in deregulation of multiple hematopoietic lineages in addition to osteoclast lineage. The osteopetrotic phenotype with Ostm1 expression specifically targeted to committed/mature *gl/gl* osteoclasts highlighted *gl* defect non-cell autonomous. Complementation of *gl/gl* osteopetrosis by additionally targeting Ostm1 to early hematopoietic lineages provided definitive evidence that Ostm1 is essential in early precursors to produce functional mature osteoclasts. Most importantly, these studies have identified a novel intercellular hematopoietic crosstalk mechanism.

Acknowledgments—We thank Drs. M. E. Hatten, N. Heintz, A. Veillette, and D. Roodman for materials.

REFERENCES

1. Teitelbaum, S. L., and Ross, P. (2003) *Nat. Rev. Genet.* **4,** 638–649
2. Boyle, W. J., Simonet, W. S., and Lacey, D. L. (2003) *Nature* **423,** 337–342
3. Zaidi, M. (2007) *Nat. Med.* **13,** 791–801
4. Janssens, K., and Van Hul, W. (2002) *Hum. Mol. Genet.* **11,** 2385–2393
5. Lazner, F., Gowen, M., Pavasovic, D., and Kola, I. (1999) *Hum. Mol. Genet.* **8,** 1839–1846
6. Wilson, C. J., and Vellodi, A. (2000) *Arch. Dis. Child* **83,** 449–452
7. Tolar, J., Teitelbaum, S. L., and Orchard, P. J. (2004) *N. Engl. J. Med.* **351,** 2839–2849
8. Balemans, W., Van Wesenbeeck, L., and Van Hul, W. (2005) *Calcif. Tissue Int.* **77,** 263–274
9. Helfrich, M. H. (2003) *Microsc. Res. Tech.* **61,** 514–532
10. Gerristen, E. J. A., Vossen, J., Fasth, A., Friedrich, W., Morgan, G., Padmos, A., Vellodi, A., Porras, O., O'Meara, A., Porta, F., Bordigoni, P., Cant, A., Hermans, J., Griscelli, C., and Fisher, A. (1994) *J. Pediatr.* **125,** 896–902
11. Eapen, M., Davies, S. M., Ramsay, N. K. C., and Orchard, P. J. (1998) *Bone Marrow Transplant.* **22,** 941–946
12. Sobacchi, C., Frattini, A., Guerrini, M. M., Abinun, M., Pangrazio, A., Susani, L., Bredius, R., Mancini, G., Cant, A., Bishop, N., Grabowski, P., Del Fattore, A., Messina, C., Errigo, G., Coxon, F. P., Scott, D. I., Teti, A., Rogers, M. J., Vezzoni, P., Villa, A., and Helfrich, M. H. (2007) *Nat. Genet.* **39,** 960–962
13. Sobacchi, C., Frattini, A., Orchard, P., Porras, O., Tezcan, I., Andolina, M., Babul-Hirji, R., Baric, I., Canham, N., Chitayat, D., Dupuis-Girod, S., Ellis, I., Etzioni, A., Fasth, A., Fisher, A., Gerristen, B., Gulino, V., Horwitz, E., Klamroth, V., Lanino, E., Mirolo, M., Musio, A., Matthijs, G., Nonomaya, S., Notarangelo, L. D., Ochs, H. D., Furga, A. S., Valiaho, J., van Hove, J. L. K., Vihinen, M., Vujic, D., Vezzoni, P., and Villa, A. (2001) *Hum. Mol. Genet.* **10,** 1767–1773
14. Michigami, T., Kageyama, T., Satomura, K., Yamaoka, K., Nakayama, M., and Ozono, K. (2002) *Bone* **30,** 436–439
15. Scimeca, J.-C., Quincey, D., Parinello, H., Romatet, D., Grogeorges, J., Gaudray, P., Philip, N., Fisher, A., and Carle, G. F. (2003) *Hum. Mut.* **21,** 151–157
16. Kornak, U., Kasper, D., Bösl, M. R., Kaiser, E., Schweizer, M., Schulz, A., Friedrich, W., Delling, G., and Jentsch, T. J. (2001) *Cell* **104,** 205–215
17. Chalhoub, N., Benachenhou, N., Rajapurohitam, V., Pata, M., Ferron, M., Frattini, A., Villa, A., and Vacher, J. (2003) *Nat. Med.* **9,** 399–406
18. Quarello, P., Forni, M., Barbereis, L., Defilippi, C., Campagnoli, M. F., Frattini, A., Chalhoub, N., Vacher, J., and Ramenghi, U. (2004) *J. Bone Miner. Res.* **19,** 1194–1199
19. Maranda, B., Chabot, G., Décarie, J.-C., Pata, M., Azeddine, B., Moreau, A., and Vacher, J. (2008) *J. Bone Miner. Res.* **23,** 296–300
20. Tondravi, M. M., McKercher, S. R., Anderson, K., Erdmann, J. M., Quiroz, M., Maki, R., and Teitelbaum, S. L. (1997) *Nature* **386,** 81–84

21. Rajapurohitam, V., Chalhoub, N., Benachenhou, N., Neff, L., Baron, R., and Vacher, J. (2001) *Bone* **28,** 513–523
22. Reddy, S. V., Scarcez, T., Windle, J. J., Leach, R. J., Hundley, J. E., Chirgwin, J. M., Chou, J. Y., and Roodman, G. D. (1993) *J. Bone Min. Res.* **8,** 1263–1270
23. Ferron, M., and Vacher, J. (2005) *Genesis* **41,** 138–145
24. Gong, S., Yang, X. W., Li, C., and Heintz, N. (2002) *Genome Res.* **12,** 1992–1998
25. Iscove, N. N., Sieber, F., and Whintherhalter, K. H. (1974) *J. Cell. Physiol.* **83,** 309–320
26. Davidson, D., and Veillette, A. (2001) *EMBO J.* **20,** 3414–3426
27. Cao, M. Y., Davidson, D., Yu, J., Latour, S., and Veillette, A. (1999) *J. Exp. Med.* **190,** 1527–1534
28. Kantor, A. B., and Herzenberg, L. A. (1993) *Annu. Rev. Immunol.* **11,** 501–538
29. Anderson, M. K., Hernandez-Hoyos, G., Diamond, R. A., and Rothenberg, E. V. (1999) *Development* **126,** 3133–3148
30. Yeamans, C., Wang, D.-Z., Paz-Priel, I., Torbett, B. E., Tenen, D. G., and Friedman, A. D. (2007) *Blood* **110,** 3136–3142
31. Li, Y., Okuno, Y., Zhang, P., Radomska, H. S., Chen, H.-M., Iwasaki, H., Akashi, K., Klemsk, M. J., McKercher, S. R., Maki, R. A., and Tenen, D. G. (2001) *Blood* **98,** 2958–2965
32. Okuno, Y., Huang, G., Rosenbauer, F., Evans, E. K., Radomska, H. S., Iwasaki, H., Akashi, K., Moreau-Gachelin, F., Li, Y., Zhang, P., Göttgens, B., and Tenen, D. G. (2005) *Mol. Cell. Biol.* **25,** 2832–2845
33. Rosenbauer, F., Owens, B. M., Yu, L., Tumang, J. R., Steidl, U., Kutok, J. L., Clayton, L. K., Wagner, K., Scheller, M., Iwasaki, H., Liu, C., Hackanson, B., Akashi, K., Leutz, A., Rothstein, T. L., Plass, C., and Tenen, D. G. (2006) *Nat. Genet.* **38,** 27–37
34. Hayase, Y., Muguruma, Y., and Lee, M. Y. (1997) *Exp. Hematol.* **25,** 19–25
35. Menaa, C., Kurihara, N., and Roodman, G. D. (2000) *Biochem. Biophys. Res. Commun.* **267,** 943–946
36. Tagaya, H., Kunisada, T., Yamazaki, H., Yamane, O., Tokuhisa, T., Wagner, E. F., Sudo, T., Shultz, L. D., and Hayashi, S.-I. (2000) *Blood* **95,** 3363–3370
37. Blin-Wakkach, C., Wacchach, A., Sexton, P. M., Rochet, N., and Carle, G. F. (2004) *Leukemia* **18,** 1505–1511
38. Nilsson, S. K., and Bertoncello, I. (1994) *Dev. Biol.* **164,** 456–462
39. Li, Y., Toraldo, G., Li, A. G., Yang, X., Zhang, H., Qian, W.-P., and Weitzmann, M. N. (2007) *Blood* **109,** 3839–3848
40. Allende, M. L., Dreier, J. L., Mandala, S., and Proia, R. L. (2004) *J. Biol. Chem.* **279,** 15396–15401
41. Lange, P., Wartosch, L., Jentsch, T., and Fuhrmann, J. (2006) *Nature* **440,** 220–223
42. Kasper, D., Planells-Cases, R., Fuhrmann, J. C., Scheel, O., Zeitz, O., Ruether, K., Schmitt, A., Poët, M., Steinfeld, R., Schweizer, M., Kornak, U., and Jentsch, T. J. (2005) *EMBO J.* **24,** 1079–1091
43. Walker, D. G. (1975) *Science* **190,** 784–785
44. Nutt, S. L., and Kee, B. L. (2007) *Immunity* **26,** 715–725
45. Lorenzo, J. (2000) *J. Clin. Invest.* **106,** 749–752
46. Weitzmann, M. N., and Pacifici, R. (2005) *Immunol. Rev.* **208,** 154–168